Inorganic Chemistry

Article

pubs.acs.org/IC

Ba_2HgS_5—A Molecular Trisulfide Salt with Dumbbell-like $(HgS_2)^{2-}$ Ions

Saiful M. Islam,[†] Jino Im,[‡] Arthur J. Freeman,[‡] and Mercouri G. Kanatzidis*[,†]

[†]Department of Chemistry and [‡]Department of Physics and Astronomy, Northwestern University, Evanston, Illinois 60208, United States

Supporting Information

ABSTRACT: Ba_2HgS_5 was synthesized by cooling a molten mixture of BaS, HgS, and elemental sulfur. It crystallizes in the orthorhombic *Pnma* space group with $a = 12.190(2)$ Å, $b = 8.677(2)$ Å, $c = 8.371(2)$ Å, and $d_{calc} = 4.77$ g cm^{-3}. Its crystal structure consists of isolated dumbbell-shaped $(HgS_2)^{2-}$ and v-shaped S_3^{2-} ions. These molecular anions are charge-balanced by Ba^{2+} cations. Raman spectroscopy shows three strong bands originating from symmetric, asymmetric, and bending vibrational modes of the S_3^{2-} ions. X-ray photoelectron spectroscopic analysis confirms the presence of the trisulfide species. Ba_2HgS_5 has a bandgap of ∼2.4 eV. Electronic band structure calculations show that the bandgap is defined essentially by the p-orbitals of the sulfur atoms of the S_3^{2-} group.

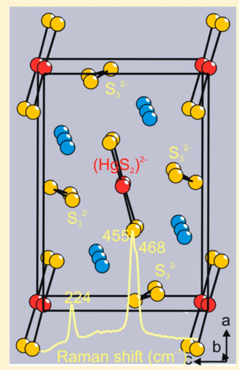

INTRODUCTION

Metal chalcogenides are key materials in many technological applications, such as hard radiation detection,[1,2] catalysis,[3] sensors,[4] electronics and optoelectronics,[5] solar energy conversion,[6] superconductivity,[7] nonlinear optics,[8] thermoelectric energy conversion,[9] topological insulators,[10] phase-change data storage,[11] and many others. This class of compounds adopts astonishingly diverse crystal structures, and this variety is partly related to the ability to form chalcogen−chalcogen bonds.[12] These bonding features are prominent for the binary alkali and alkaline-earth metal chalcogenides. The anionic polychalcogenide units in A_2Q_2 (A = Na, K, Rb, Cs; Q = S, Se),[13−15] A_2Q_3 (A = K, Rb, Cs; Q = S, Se, Te),[16−19] A_2Q_5 (A = K, Rb, Cs; Q = S, Se, Te),[20−22] Cs_2S_6,[23,24] BaQ_2 (Q = S, Se),[25−27] BaQ_3 (Q = S, Se),[26,28] SrS_2,[26] and SrS_3[26] are stabilized by charge balancing from the metal cation. The use of alkali metal polychalcogenide fluxes have been very effective in the discovery of numerous ternary polychalcogenides.[12a,29] Interestingly, despite the existence of several ternary alkali polychalcogenides of Au,[12a,30] Ag,[31]and Cu,[12a] their isoelectronic cadmium and mercury cations tend to form only monochalcogenides. Among the main group elements, mercury exhibits a substantially larger polarizibility as well as diverse coordination preferences and forms a plethora of compounds.[12a,32] In the ternary system, A/Hg/Q (A = alkali/alkaline earth metals; Q = chalcogens), A_6HgQ_4 (A = K, Rb; Q = S, Se),[33] $A_2Hg_3Q_4$ (A = K, Na; Q = S, Se),[34,35] $Na_2Hg_3S_4$,[36] $Rb_2Hg_3Te_4$,[37] $A_2Hg_6Q_7$ (A = K, Rb, Cs; Q = S, Se),[34] A_2HgS_2 (A = Na, K),[38] $BaHgS_2$,[39] and Ba_2HgS_3[40] have been reported. In these compounds, only Q^{2-} exist, which are exclusively bonded with the Hg^{2+} cations forming $(Hg_xQ_y)^{n-}$ groups, and are charged-balanced by counter metal cations. From this observation one can easily surmise that the very strong affinity of the Hg^{2+} cations toward the Q^{2-} anions may hinder the stabilization of polysulfide groups in its alkali/alkaline earth metal compounds.

Here, we report an exception to this trend, namely, the synthesis of Ba_2HgS_5, the first polysulfide in the system A/Hg/Q, (A = alkali/alkaline-earth metals; Q = chalcogenides). It is a double salt of the molecular anions of $(HgS_2)^{2-}$ and S_3^{2-}, which are counterbalanced by Ba^{2+} cations. The presence of the S_3^{2-} group is further supported by Raman spectroscopy. In addition, we show that X-ray photoelectron spectroscopy can well-distinguish the multiple oxidation states of sulfur atoms in the compound. This new ternary polysulfide is a wide bandgap semiconductor with a bandgap of ∼2.4 eV. According to first-principles electronic band structure calculations, the origin of the bandgap is mainly the S_3^{2-} polysulfide group.

EXPERIMENTAL SECTION

Reagent. BaS, elemental sulfur, and mercury were obtained commercially from alpha aldrich (99.5%), 5N Plus Inc., and Sigma-Aldrich (99.9999%), respectively. HgS was synthesized in the laboratory by slowly heating a stoichiometric mixture of elemental mercury and sulfur to 600 °C for 24 h, soaking it for 12 h, and cooling it to room temperature in 24 h. ***Caution!*** *Hg is highly toxic, and great care should be exerted with appropriate protective equipment in both the synthesis and handling of the* Ba_2HgS_5.

Synthesis of Ba_2HgS_5. Microcrystalline powder of barium dithio(trithio)mercurate(II) was obtained by cooling a melted mixture of BaS, (169 mg, 1 mmol), HgS (232 mg, 1 mmol), and elemental sulfur (69 mg, 2.2 mmol). For the synthesis, a homogeneous mixture

Received: February 17, 2014
Published: April 10, 2014

of the starting materials was transferred into a carbon-coated silica tube, which was flame-sealed under vacuum (10^{-4} mbar). Subsequently, the tube was heated to 575 °C in 48 h, soaked isothermally for 12 h, and then slowly cooled to 300 °C in 67 h, followed by cooling to room temperature in 3 h. During this heating process the sample-containing end of the sealed tube ($l \approx 13$ cm, $d \approx 0.9$ cm) was placed at the center of a tube furnace, while the empty end was closer to the end of the furnace. This, in practice, led to a temperature gradient for the reaction. Thus, Ba_2HgS_5 (main phase) and some unknown compounds were formed at the center of the furnace (higher temperature) with a yield of about 75%, while the empty end (lower temperature) contained a mixture of HgS and a trace of elemental sulfur.

To optimize the synthesis, a stoichiometric mixture of BaS, HgS, and elemental sulfur was heated in a smaller tube ($l \approx 8$ cm, $d \approx 0.9$ cm). To prevent a larger diffusion of HgS and S from the reaction mixtures, the sealed tube was placed in the furnace so that the empty end of the tube was at the center of the furnace 650 °C (higher temperature), and the above heating procedure was applied. This procedure led to the formation of mainly Ba_2HgS_5 along with a small amount of $BaHgS_2$ and traces of black HgS. Yellow irregular-shaped single crystals up to 0.1 mm in edge length were obtained from presynthesized Ba_2HgS_5 (~500 mg; contaminated with traces of HgS and $BaHgS_2$) by heating to 650 °C in 12 h, soaking isothermally for 24 h, cooling to 500 °C in 6 h, and holding there for 6 h. Finally, the sample was slowly cooled to 300 °C in 72 h, followed by cooling to room temperature in 3 h. This experiment gave the compound in 93% yield.

Powder X-ray Diffraction. Powder X-ray diffraction (PXRD) data were collected on ground crystalline samples of each product with a flat sample geometry using a silicon-calibrated CPS 120 INEL powder X-ray diffractometer (Cu Kα graphite-monochromatized radiation) operating at 40 kV and 20 mA equipped with a position-sensitive detector. Simulated patterns were generated using the CIF of each refined structure and the Visualizer program within FindIt.

Scanning Electron Microscopy. Images and semiquantitative energy-dispersive X-ray spectroscopy (EDS) analyses were obtained using a Hitachi S-3400 scanning electron microscope equipped with a PGT energy-dispersive X-ray analyzer. Spectra were collected using an accelerating voltage of 15 kV and a 90 s accumulation time.

Single-Crystal X-ray Crystallography. Data collections were performed on a STOE IPDS II diffractometer using Mo Kα radiation (λ = 0.710 73 Å) operating at 50 kV and 40 mA at 293 K. Integration and numerical absorption corrections were performed using X-AREA, X-RED, and X-SHAPE. The structure was solved using direct methods and refined by full-matrix least-squares on F^2 using the SHELXTL program package.[41] A complete list of crystallographic information, data collection, structure refinement, atomic coordinates, and isotropic displacement parameters are given in Tables 1 and 2.

Ultraviolet−Visible Spectroscopy. Diffuse reflectance spectra of the selected crystals of Ba_2HgS_5 were collected in the range of 200−2500 nm using a Shimadzu UV-3101 PC double-beam, double-monochromator spectrophotometer. The instrument was equipped with an integrating sphere and controlled by a personal computer. $BaSO_4$ was used as a standard and set to 100% reflectance. Samples were prepared by placing ground crystalline products on a bed of $BaSO_4$. Collected reflectance data were converted to absorbance according to the Kubelka−Munk equation: $\alpha/S = (1 - R)^2/(2R)$, where R is the reflectance and α and S are the absorption and scattering coefficients, respectively.[42] The band gap was determined as the intersection point between the energy axis and the line extrapolated from the linear portion of the absorption edge in an $(\alpha/S)^2$ versus E plot.

Raman Spectroscopy. The Raman spectrum of the crushed crystals of Ba_2HgS_5 was collected on a DeltaNu Advantage NIR spectrometer equipped with a CCD detector using 785 nm radiation from a diode laser. The samples were loaded into borosilicate glass capillaries for the measurement. A maximum power of 60 mW and beam diameter of 35 μm were used. The spectrum was collected using an integration time of 15 s.

Table 1. Details Concerning Data Collection and Structure Refinement of Ba_2HgS_5

crystal data	Ba_2HgS_5
crystal system	orthorhombic
space group	*Pnma* (62)
color	yellow
a/Å	12.190(2)
b/Å	8.677(2)
c/Å	8.371(2)
V/Å^3	885.37(3)
Z	4
μ/mm^{-1}	27.18
$\rho_{X\text{-ray}}$/g cm^{-3}	4.77
color	yellow
crystal shape	rectangular
size/mm^3	0.03 × 0.01 × 0.007
MW/g mol^{-1}	635.6
F(000)	1087.7
data collection	
Mo Kα radiation	λ = 0.710 73 Å
monochromator	graphite
temperature/K	293
scan range θ/deg	$3 \le \theta \le 30$
	$0 \le h \le 17$
	$-12 \le k \le 0$
	$-11 \le l \le 11$
structure refinement software	SHELX97[41]
measured reflections	3886
independent reflections	1369
parameters; GOF	44; 0.88
residuals	
R_{int}	0.020
$R_1{}^a$	0.020
$R_{1all}{}^a$	0.032
$wR_2{}^b$	0.028
extinction coefficient	0.001 36
weighting scheme	A = 0.0089; B = 0.0
res. electron density	
$\Delta\rho_{max}$/Å^{-3}	1.46 (close to S2)
$\Delta\rho_{min}$/Å^{-3}	2.12 (close to Ba1)

$^aR_1 = \Sigma||F_0| - |F_c||/|F_0|$, $F_0^2 \ge 2\sigma(F_0^2)$ $^bwR_2 = 1/[\sigma^2(F_0^2) + (A \times P)^2 + B \times P]$; $P = (F_0^2 + 2F_c^2)/3$

X-ray Photoelectron Spectroscopy. X-ray photoelectron studies of the crushed crystals of Ba_2HgS_5 were performed using a Thermo Scientific ESCALAB 250 Xi spectrometer equipped with a monochromatic Al Kα X-ray source (1486.6 eV) and operated at 300 W. Samples were analyzed under vacuum ($P < 10^{-9}$ mbar), where survey scans and high-resolution scans were collected using a pass energy of 150 and 25 eV, respectively. Binding energies were referred to the C 1s binding energy at 284.6 eV. A low-energy electron flood gun was employed for charge neutralization. Prior to X-ray photoelectron spectroscopy (XPS) measurements, the crystalline powders were pressed on copper foil, mounted on stubs, and successively put into the entry-load chamber to pump.

Band Structure Calculations. To investigate the electronic structure of Ba_2HgS_5, first-principles calculations were performed within the density functional theory formalism using the projector augmented wave method[43] implemented in Vienna Ab-initio Simulation Package.[44,45] The energy cutoff for plane wave basis was set to 350 eV and 12 × 12 × 8 k-point mesh was chosen for Brillouin zone sampling. For exchange-correlation functional, the generalized gradient approximation (GGA) was employed within the Perdew−Burke−Ernzerhof (PBE) formalism.[46] The experimentally observed

Table 2. Atomic Coordinates and Isotropic Displacement Parameters for Ba_2HgS_5

atoms	Wyck.	S.O.F.	x	y	z	δ_{iso}
Hg1	4*c*	0.5	0.00896(2)	1/4	0.98781(3)	0.01779(7)
Ba1	8*d*	1.0	−0.18950(2)	0.00671(3)	0.35649(3)	0.01178(6)
S1	4*c*	0.5	0.0264(1)	1/4	0.4327(2)	0.0144(3)
S2	4*c*	0.5	0.1938(1)	1/4	0.9091(2)	0.0134(3)
S3	4*c*	0.5	−0.1771(1)	1/4	1.05646(2)	0.0136(3)
S4	8*d*	1.0	0.06742(9)	0.0513(1)	0.3046(1)	0.0156(2)

crystal structure was used for the electronic band structure calculations.

■ RESULTS AND DISCUSSION

Synthesis. $BaHgS_2$ (crimson red) and Ba_2HgS_3 (bright red) were synthesized from a stoichiometric mixture of their corresponding sulfides at 400−850 °C.[40,39] On the other hand, the synthesis of Ba_2HgS_5 (yellow) can be achieved from reacting a mixture of BaS, HgS, and elemental sulfur in closed silica ampule under 650 °C. The formation of Ba_2HgS_5 is fairly reproducible; however, often intermingled impurities are of black HgS and trace amounts of unknown compounds. Black HgS formed, presumably by the deposition from the gas phase during the cooling step. The difficulty in obtaining a single phase of Ba_2HgS_5 is because both HgS and S easily sublime and separate themselves from the reaction mixture. Using an excess of HgS can produce Ba_2HgS_5 (∼90% phase purity, visual inspection under microscope) as the main phase. A comparison between the calculated and experimental X-ray diffraction pattern is shown in Figure 1. This compound is soluble in polar organic solvents such as formamide and *N*-methylformamide but is insoluble in dimethylformamide and acetone.

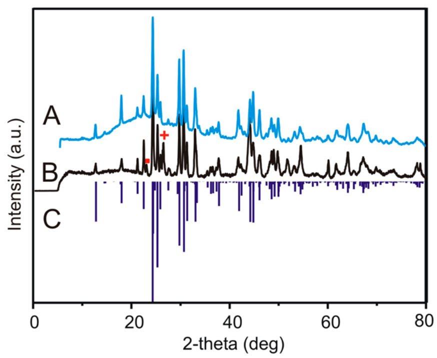

Figure 1. X-ray powder diffraction of (A) selected crystals, (B) impurity highlighted, and (C) calculated patterns of Ba_2HgS_5. Red cross indicates impurity from HgS (other peaks overlap with Ba_2HgS_5), and red circles indicate impurity from an unknown phase.

Crystal Structure. Ba_2HgS_5 crystallizes in the orthorhombic space group *Pnma*. The asymmetric unit in Ba_2HgS_5 consists of one Ba, one Hg, and four S atoms (Tables 2 and 3). The unique crystal structure of Ba_2HgS_5 is composed of isolated dumbbell-shaped $(HgS_2)^{2-}$ anions and v-shaped S_3^{2-} units, which are charge-balanced by Ba^{2+} cations, forming a mixed anion molecular salt compound (Figure 2). The presence of discrete S_3^{2-} ions in Ba_2HgS_5 is a remarkable feature of this compound. The monosulfide anions S^{2-} have 5-fold coordination with four Ba^{2+} and one Hg^{2+} atoms, forming a square pyramid. The atoms of the S_3^{2-} group exhibit two different types of coordination; the terminal $S^{1-}(1)$ ions have 4-fold coordination ($3Ba^{2+}$ and S^{o}), while the internal $S^{o}(4)$ atoms possess 6-fold coordination ($4Ba^{2+}$ and $2S^{1-}$) (Figure 3). The interaction of S^{o} with Ba^{2+} ions is comparatively weak, and $Ba^{2+}-S^{o}$ bond distances of ∼3.45 Å are observed. The S−S−S angle is 111.12°, which is in agreement with other S_3^{2-} ions.[26] Hg^{2+} exhibits 2-fold coordination only with S^{2-} ions, and thus the Hg^{2+} cation is encapsulated, leaving the S_3^{2-} ion discrete. In contrast to the structural features of Ba_2HgS_5, both Ba_2HgS_3[40] and $BaHgS_2$[39] exhibit only S^{2-} units, which are exclusively bonded to Hg^{2+} cations. The former exhibit only $[HgS_4]$ tetrahedra, and the latter consists of $[HgS_4]$ tetrahedra and linearlike $[HgS_2]$ units.

Selected interatomic distances and angles are depicted in Figure 3 and Table 3. The interatomic distance d(S1−S4) = 2.09 Å, of the S_3^{2-} group in Ba_2HgS_5, is in agreement with other S_3^{2-} units.[16,17] Hg−S bond distances of ∼2.34 Å and linearlike S−Hg−S angles, <(S3−Hg1−S2) = 177.9°, in $(HgS_2)^{2-}$ are in agreement with other compounds featuring linearlike S−Hg−S units such as $BaHgS_2$[39] and $Cs_2Hg_3M_2S_8$ (M = Sn, Ge).[47]

Raman Spectrum. Optical Raman spectroscopic analysis (Figure 4) confirms the presence of S−S bonds. Two strong peaks at 455 and 468 cm^{-1} and a weaker peak at 224 cm^{-1} are

Table 3. Selected Interatomic Distances (Å) and Angles (deg) in Ba_2HgS_5[a]

d(Hg1—S3)	2.339(2)	d(S1—S4)	2.091(1)	∠(S3—Hg1—S2)	177.91(6)
d(Hg1—S2)	2.347(2)	d(S1—Ba1)	3.434(1)	∠(S4—S1—S4)	111.13(9)
d(Ba1—S2)	3.148(1)	d(S1—Ba1)	3.468(1)	∠(S2—Ba1—S2)	152.71(2)
d(Ba1—S4)	3.185(1)	d(S2—Ba1)	3.148(1)	∠(S2—Ba1—S4)	121.05(3)
d(Ba1—S2)	3.214(1)	d(S2—Ba1)	3.214(1)	∠(Ba1—S1—Ba1)	158.23(5)
d(Ba1—S3)	3.226(1)	d(S3—Ba1)	3.226(1)	∠(Ba1—S1—Ba1)	97.99(2)
d(Ba1—S4)	3.243(1)	d(S3—Ba1)	3.285(1)	∠(S4—S1—Ba1)	65.23(4)
d(Ba1—S4)	3.279(1)	d(S4—Ba1)	3.243(1)	∠(S4—S1—Ba1)	126.52(7)
d(Ba1—S3)	3.285(1)	d(S4—Ba1)	3.279(1)	∠(S3—Ba1—S4)	70.77(4)
d(Ba1—S1)	3.434(1)	d(Ba1—Ba1)	4.222(1)	∠(S2—Ba1—S4)	77.17(3)
d(Ba1—S1)	3.4682(1)	d(Ba1—Ba1)	4.4392(8)	∠(S4—Ba1—S4)	144.91(2)

[a]Estimated standard deviation in parentheses.

dx.doi.org/10.1021/ic500388s | *Inorg. Chem.* 2014, 53, 4698−4704

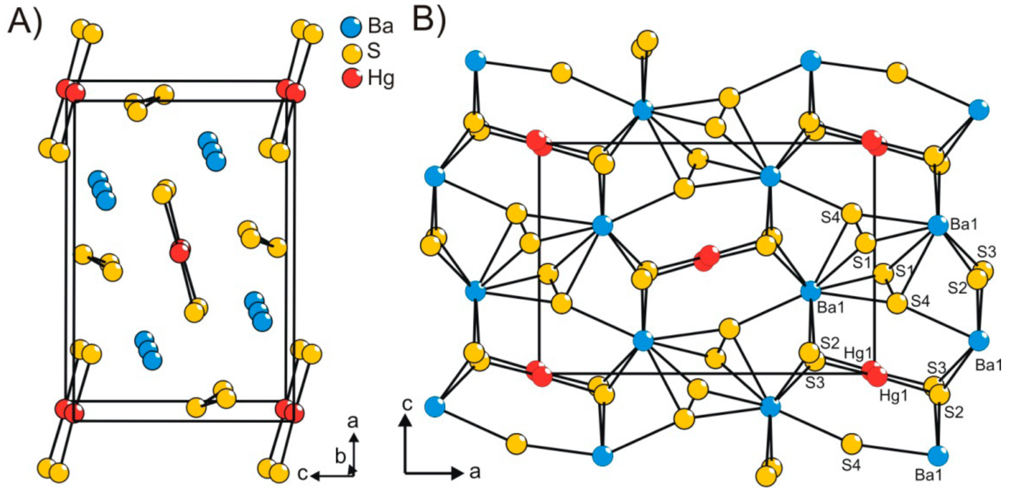

Figure 2. Different views of the crystal structure of Ba_2HgS_5; (A) isolated linearlike $(HgS_2)^{2-}$, v-shaped S_3^{2-}, and Ba^{2+} ions; (B) connectivity of the isolated anions by interstitial Ba^{2+} cations. The Ba···S interactions are drawn.

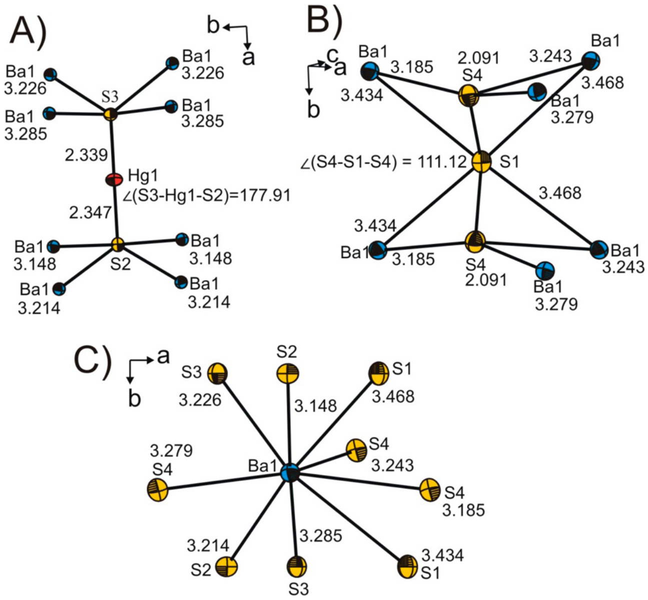

Figure 3. Coordination environments of the three different types of atoms in Ba_2HgS_5. Ellipsoids are at 70% probability limit.

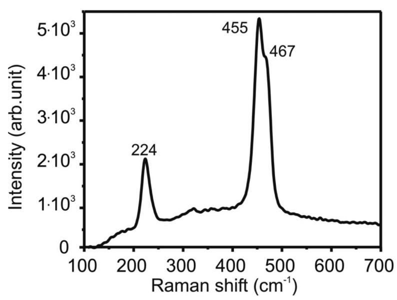

Figure 4. Room-temperature Raman spectrum of Ba_2HgS_5.

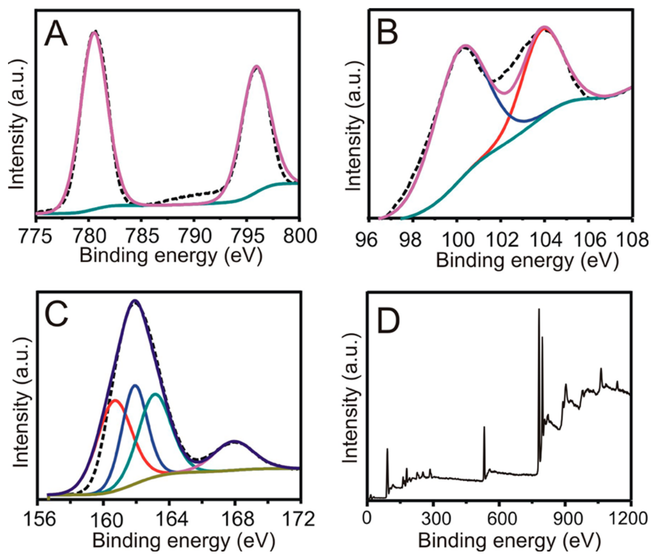

Figure 5. X-ray photoelectron spectra of (A) barium, (B) mercury, (C) sulfur, and (D) survey spectrum for Ba_2HgS_5. Hatched and solid lines represent experimental and deconvoluted spectra, respectively.

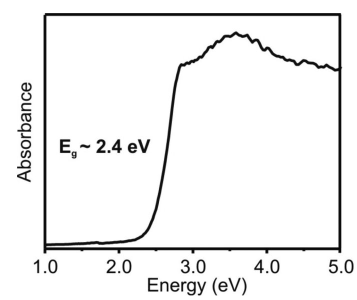

Figure 6. UV−vis optical absorption spectrum of solid Ba_2HgS_5.

observed. In agreement with Jang et al.,[48] we assign these three peaks as symmetric, asymmetric, and bending vibrational modes for C_{2v} symmetry of S_3^{2-} free ions in Ba_2HgS_5. Apart from this, a very weak peak at ~323 cm^{-1} might be attributed to mercury−sulfur vibrations. Other peaks from $(HgS_2)^{-2}$, if any, might be superimposed with the low-energy broad peak at 224 cm^{-1}.

X-ray Photoelectron Spectroscopy. Ba_2HgS_5 was analyzed by X-ray photoelectron spectroscopy (Figure 5). Peaks at 795.78 and 780.68 eV are characteristic for $3d_{3/2}$ and $3d_{5/2}$ barium(II) cations (Figure 5a).[49] Peaks at about 100.15 and 103.68 eV essentially provide confirmation of $4f_{5/2}$ and $4f_{7/2}$

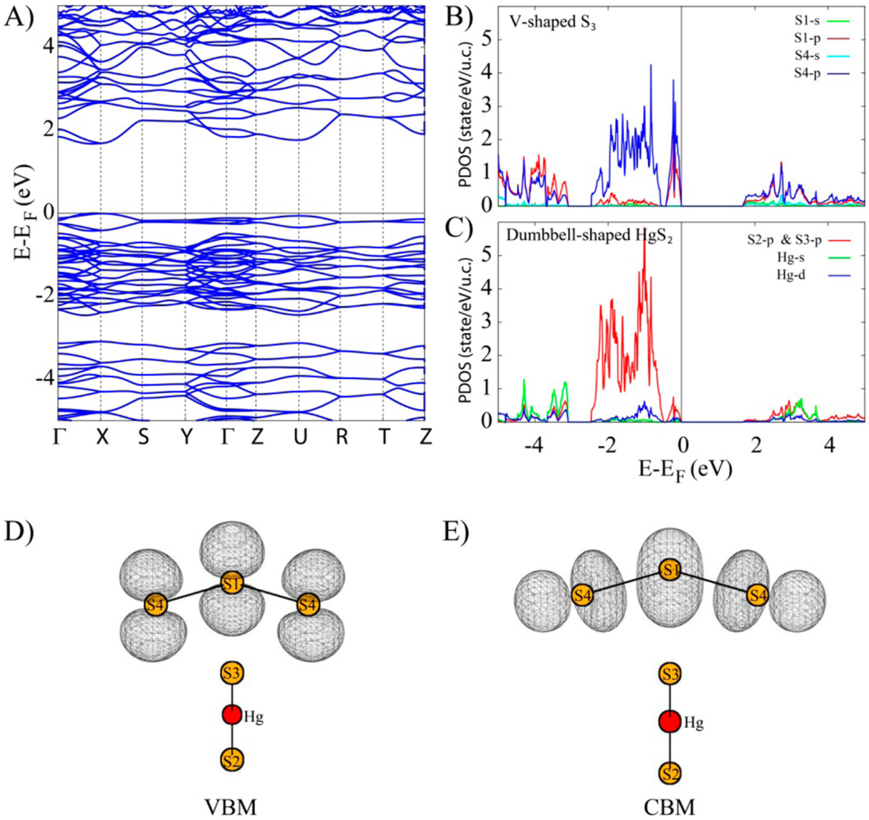

Figure 7. (A) Electronic band structure of Ba_2HgS_5, (B) projected density of states (PDOS) of the S_3 chainlike unit, (C) PDOS of the HgS_2 unit, (D) real space projection of VBM, (E) real space projection of CBM. In (B), green, red, light blue, and blue lines correspond to the s-orbitals of S1, p-orbitals of S1, s-orbitals of S4, and p-orbitals of S4, respectively. In (C), red, green, and blue lines indicate the p-orbitals of S2 and S3, s-orbitals of Hg, and d-orbitals of Hg, respectively. In (D) and (E), isosurfaces of the square of absolute value of the wave function at VBM and CBM are plotted by black wireframes, respectively.

from Hg^{2+} ions (Figure 5b).[50] The XPS of sulfur essentially shows two bands; the lower-energy band from ~160−165 eV and the higher-energy band centered at 167.98 eV (Figure 5c). These bands correspond to the sulfur 2p energies.[51,52] Deconvolution of the broad band in the 160−165 eV range gives three bands centered at 160.83, 161.72, and 163.19 eV. These bands originate from S 2p of S^{2-}, S^{1-}, and S°. The band centered at 167.98 eV is the signature for sulfur 2p from SO_4^{2-}[52], which likely originates from the partial oxidation of the surface sulfur atoms of the polysulfide groups (S_3^{2-}). The band at ~531 eV is in agreement with the O 2p energies that further confirms the formation of sulfate ions.[53]

Optical Properties. The electronic absorption spectrum determined from optical diffuse reflectance data of pure Ba_2HgS_5 shows a bandgap of 2.4 eV (Figure 6). This bandgap is consistent with its yellow color. The sharp character of the absorption edge is suggestive of a direct electronic transition, and this is supported by electronic band structure calculations below. By comparison, the bandgap of $BaHgS_2$ is ~1.94 eV (unpublished results).

Electronic Structure. To understand the nature of the bandgap of Ba_2HgS_5, we calculated the electronic band structure and the projected density of states (PDOS). The electronic band structure in Figure 7a shows that Ba_2HgS_5 has a direct band gap near the X-point between X and S. The bandgap is predicted to be 1.7 eV with the PBE exchange-correlation functional, which is underestimated compared to the experimental bandgap of 2.4 eV. This is a well-known tendency of semilocal functional like GGA.[54,55]

From the PDOS calculations, we find that both the conduction band minimum (CBM) and valence band maximum (VBM) mainly originate from the S_3^{2-} ions. In Figure 7b,c, we plot the PDOS of the S_3^{2-} ions and the dumbbell-shaped $(HgS_2)^{2-}$, respectively. As shown in Figure 7b, the VBM consists mainly of p-orbitals of S1 and S4, and the CBM is composed of s- and p-orbitals of S1 and p-orbitals of S4. To depict the interaction between orbitals of the S_3^{2-} ions, we calculated the real space projection of the square of the absolute value of wave functions at the VBM and CBM. Figure 7d,e shows that the wave function at the VBM consists of p-orbitals of S1 and S4, which are perpendicular to the S1−S4 bonding direction, while at the CBM p-orbitals of S4 and sp hybridized orbitals of S1 interact along the S1−S4 bonding direction. It indicates that the VBM and CBM originate from the π-like state and the σ-like state of the S_3^{2-} ions, respectively. On the other hand, as shown in Figure 7c, the electronic states of the $(HgS_2)^{2-}$ ions have a relatively small contribution to the VBM and almost no contribution to the CBM. Instead, the lone-pair states of p-orbitals of S2 and S3 are distributed from −3.5 eV to −0.5 eV with respect to the Fermi level. Bonding and antibonding states between p-orbitals of S2/S3 and ds hybridized states of Hg are located around −4 and 3 eV, respectively. These results confirm our intuitive view that the best way to visualize this material is as a molecular salt akin to other simple salts like BaS_3[26]and K_2S_3.[16]

■ CONCLUDING REMARKS

Ba_2HgS_5 is a rare type of mixed molecular salt with linear complexes of $(HgS_2)^{2-}$, v-shaped S_3^{2-} ions, and interstitial Ba^{2+} cations. Raman and X-ray photoelectron spectroscopy provide additional evidence for the presence of the polysulfide group. Electronic structure calculations reveal that this molecular salt has a direct band, which is in agreement with the sharp absorption edge observed in the optical spectrum. This calculation shows that the origin of the VBM and CBM extrema is mainly the s- and p-orbitals of the sulfur atoms in the S_3^{2-} ions forming π-like and σ-like states, respectively. Although, technically Ba_2HgS_5 is a polysulfide compound, the fact that Hg does not bind directly to the polysulfide anion is consistent with the known mercury chalcogenide chemistry where no polysulfide compound exists. In this regard it is different from the Cu, Ag, and Au chemistry and in sharp contrast to the rich polychalcogenide chemistry of mercury known in molecular complexes.[56]

■ ASSOCIATED CONTENT

Supporting Information

X-ray crystallographic file (CIF), crystallographic refinement details, atomic coordinates with equivalent isotropic displacement parameters, anisotropic displacement parameters, and selected bond distances for Ba_2HgS_5. This material is available free of charge via the Internet at http://pubs.acs.org.

■ AUTHOR INFORMATION

Corresponding Author

*E-mail: m-kanatzidis@northwestern.edu.

Author Contributions

The manuscript was written through contributions of all authors. All authors have given approval to the final version of the manuscript.

Notes

The authors declare no competing financial interest.

■ ACKNOWLEDGMENTS

This research was supported by the National Science Foundation Grant DMR-1104965. SEM and EDS analyses were performed at the EPIC facility of the NUANCE Center at Northwestern University, supported by NSF-NSEC, NSF-MRSEC, Keck Foundation, the State of Illinois, and Northwestern University. The electronic structure calculations we supported by a DTRA grant (HDTRA1 09-1-0044).

■ REFERENCES

(1) Owens, A. *J. Synchrotron Radiat.* **2006**, *13*, 143−50.

(2) (a) Androulakis, J.; Peter, S. C.; Li, H.; Malliakas, C. D.; Peters, J. A.; Liu, Z.; Wessels, B. W.; Song, J. H.; Jin, H.; Freeman, A. J.; Kanatzidis, M. G. *Adv. Mater.* **2011**, *23*, 4163−7. (b) Johnsen, S.; Liu, Z.; Peters, J. A.; Song, J. H.; Nguyen, S.; Malliakas, C. D.; Jin, H.; Freeman, A. J.; Wessels, B. W.; Kanatzidis, M. G. *J. Am. Chem. Soc.* **2011**, *133*, 10030−3. (c) Li, H.; Peters, J. A.; Liu, Z. F.; Sebastian, M.; Malliakas, C. D.; Androulakis, J.; Zhao, L. D.; Chung, I.; Nguyen, S. L.; Johnsen, S.; Wessels, B. W.; Kanatzidis, M. G. *Cryst. Growth Des.* **2012**, *12*, 3250−3256. (d) Nguyen, S. L.; Malliakas, C. D.; Peters, J. A.; Liu, Z. F.; Im, J.; Zhao, L. D.; Sebastian, M.; Jin, H.; Li, H.; Johnsen, S.; Wessels, B. W.; Freeman, A. J.; Kanatzidis, M. G. *Chem. Mater.* **2013**, *25*, 2868−2877.

(3) (a) Bag, S.; Gaudette, A. F.; Bussell, M. E.; Kanatzidis, M. G. *Nat. Chem.* **2009**, *1*, 217−224. (b) Bag, S.; Trikalitis, P. N.; Chupas, P. J.; Armatas, G. S.; Kanatzidis, M. G. *Science* **2007**, *317*, 490−493. (c) Chianelli, R. R.; Daage, M.; Ledoux, M. J. *Adv. Catal.* **1994**, *40*, 177−232. (d) Prins, R.; Debeer, V. H. J.; Somorjai, G. A. *Catal. Rev.* **1989**, *31*, 1−41. (e) Yuhas, B. D.; Smeigh, A. L.; Samuel, A. P. S.; Shim, Y.; Bag, S.; Douvalis, A. P.; Wasielewski, M. R.; Kanatzidis, M. G. *J. Am. Chem. Soc.* **2011**, *133*, 7252−7255.

(4) (a) Eggleton, B. J.; Luther-Davies, B.; Richardson, K. *Nat. Photonics* **2011**, *5*, 141−148. (b) Mizaikoff, B.; Gobel, R.; Krska, R.; Taga, K.; Kellner, R.; Tacke, M.; Katzir, A. *Sens. Actuators, B* **1995**, *29*, 58−63.

(5) (a) Beal, A. R.; Hughes, H. P.; Liang, W. Y. *J. Phys. C: Solid State Phys.* **1975**, *8*, 4236−4248. (b) Terrones, H.; Lopez-Urias, F.; Terrones, M. *Sci. Rep.* **2013**, *3*, 1549;. (c) Wang, Q. H.; Kalantar-Zadeh, K.; Kis, A.; Coleman, J. N.; Strano, M. S. *Nat. Nanotechnol.* **2012**, *7*, 699−712.

(6) (a) Fontana, M.; Deppe, T.; Boyd, A. K.; Rinzan, M.; Liu, A. Y.; Paranjape, M.; Barbara, P. *Sci. Rep.* **2013**, *3*;. (b) Jäger-Waldau, A.; Lux-Steiner, M. C.; Bucher, E. *Solid State Phenom.* **1994**, *37−38*, 479.

(7) (a) Fisher., Ø., Maple, M. B. *Topics in Current Physics: Superconductivity in Ternary Compounds I;* Springer-Verlag: Berlin, Germany, 1982. (b) Hampshire, D. P. *Handbook of Superconducting Materials,* Taylor & Francis: Vol. 2; 2002. (c) Maaren, M. H. v.; Schaeffer, G. M. *Phys. Lett.* **1966**, *20*. (d) Yvon, K. I. *Current Topics in Material Science;* Elsevier: North-Holland, Amsterdam, 1979; Vol. 3. (e) Zhang, Y.; Yang, L. X.; Xu, M.; Ye, Z. R.; Chen, F.; He, C.; Xu, H. C.; Jiang, J.; Xie, B. P.; Ying, J. J.; Wang, X. F.; Chen, X. H.; Hu, J. P.; Matsunami, M.; Kimura, S.; Feng, D. L. *Nat. Mater.* **2011**, *10*, 273−7.

(8) (a) Chen, M. C.; Wu, L. M.; Lin, H.; Zhou, L. J.; Chen, L. *J. Am. Chem. Soc.* **2012**, *134*, 6058−60. (b) Chung, I.; Jang, J. I.; Malliakas, C. D.; Ketterson, J. B.; Kanatzidis, M. G. *J. Am. Chem. Soc.* **2010**, *132*, 384−9. (c) Chung, I.; Kanatzidis, M. G. *Chem. Mater.* **2014**, *26*, 849−869. (d) Isaenko, L.; Yelisseyev, A.; Lobanov, S.; Petrov, V.; Rotermund, F.; Slekys, G.; Zondy, J. J. *J. Appl. Phys.* **2002**, *91*, 9475−9480. (e) Liao, J. H.; Marking, G. M.; Hsu, K. F.; Matsushita, Y.; Ewbank, M. D.; Borwick, R.; Cunningham, P.; Rosker, M. J.; Kanatzidis, M. G. *J. Am. Chem. Soc.* **2003**, *125*, 9484−93. (f) Vogel, E. M.; Weber, M. J.; Krol, D. M. *Phys. Chem. Glasses* **1991**, *32*, 231.

(9) (a) Biswas, K.; He, J.; Zhang, Q.; Wang, G.; Uher, C.; Dravid, V. P.; Kanatzidis, M. G. *Nat. Chem.* **2011**, *3*, 160−6. (b) Chung, D. Y.; Hogan, T.; Brazis, P.; Rocci-Lane, M.; Kannewurf, C.; Bastea, M.; Uher, C.; Kanatzidis, M. G. *Science* **2000**, *287*, 1024−7. (c) Heremans, J. P.; Jovovic, V.; Toberer, E. S.; Saramat, A.; Kurosaki, K.; Charoenphakdee, A.; Yamanaka, S.; Snyder, G. J. *Science* **2008**, *321*, 554−7. (d) Hsu, K. F.; Loo, S.; Guo, F.; Chen, W.; Dyck, J. S.; Uher, C.; Hogan, T.; Polychroniadis, E. K.; Kanatzidis, M. G. *Science* **2004**, *303*, 818−21. (e) Kanatzidis, M. G. *Chem. Mater.* **2010**, *22*, 648−659. (f) Quarez, E.; Hsu, K. F.; Pcionek, R.; Frangis, N.; Polychroniadis, E. K.; Kanatzidis, M. G. *J. Am. Chem. Soc.* **2005**, *127*, 9177−90. (g) Sootsman, J. R.; Chung, D. Y.; Kanatzidis, M. G. *Angew. Chem., Int. Ed. Engl.* **2009**, *48*, 8616−39.

(10) (a) Hsieh, D.; Xia, Y.; Qian, D.; Wray, L.; Dil, J. H.; Meier, F.; Osterwalder, J.; Patthey, L.; Checkelsky, J. G.; Ong, N. P.; Fedorov, A. V.; Lin, H.; Bansil, A.; Grauer, D.; Hor, Y. S.; Cava, R. J.; Hasan, M. Z. *Nature* **2009**, *460*, 1101−5. (b) Koumoulis, D.; Chasapis, T. C.; Taylor, R. E.; Lake, M. P.; King, D.; Jarenwattananon, N. N.; Fiete, G. A.; Kanatzidis, M. G.; Bouchard, L. S. *Phys. Rev. Lett.* **2013**, *110*, 026602.

(11) (a) Chrissafis, K.; Kyratsi, T.; Paraskevopoulos, K. M.; Kanatzidis, M. G. *Chem. Mater.* **2004**, *16*, 1932−1937. (b) Pandey, A.; Brovelli, S.; Viswanatha, R.; Li, L.; Pietryga, J. M.; Klimov, V. I.; Crooker, S. A. *Nat. Nanotechnol.* **2012**, *7*, 792−797. (c) Pirovano, A.; Lacaita, A. L.; Benvenuti, A.; Pellizzer, F.; Bez, R. *IEEE Trans. Electron Devices* **2004**, *51*, 452−459. (d) Yamada, N.; Ohno, E.; Nishiuchi, K.; Akahira, N.; Takao, M. *J. Appl. Phys.* **1991**, *69*, 2849−2856.

(12) (a) Kanatzidis, M. G.; Sutorik, A. C. *Prog. Inorg. Chem.* **1995**, *43*, 151−265. (b) Zhang, Q. C.; Malliakas, C. D.; Kanatzidis, M. G. *Inorg. Chem.* **2009**, *48*, 10910−10912. (c) Xiong, W. W.; Li, P. Z.; Zhou, T. H.; Tok, A. I.; Xu, R.; Zhao, Y.; Zhang, Q. *Inorg. Chem.* **2013**, *52*, 4148−50.

(13) Boettcher, P.; Getzschmann, J.; Keller, R. *Z. Anorg. Allg. Chem.* **1993**, *619*, 476–488.
(14) Boettcher, P.; Keller, R. *J. Less-Common Met.* **1985**, *109*, 311–321.
(15) Getzschmann, J.; Boettcher, P. *Z. Kristallogr.* **1996**, *211*, 90–95.
(16) Boettcher, P. *Z. Anorg. Allg. Chem.* **1977**, *432*, 167–172.
(17) Boettcher, P. *Z. Anorg. Allg. Chem.* **1980**, *461*, 13–21.
(18) Chuntonov, K. A.; Orlov, A. N.; Yatsenko, S. P.; Grin, Y. N.; Miroshnikova, L. D. *Inorg. Mater.* **1982**, *18*, 941–943.
(19) Eisenmann, B.; Schafer, H. *Angew. Chem., Int. Ed.* **1978**, *17*, 684–684.
(20) Kelly, B.; Woodward, P. *J. Chem. Soc., Dalton Trans.* **1976**, 1314–1316.
(21) Boettcher, P.; Kruse, K. *J. Less-Common Met.* **1982**, *83*, 115–125.
(22) Kretschmann, U.; Bottcher, P. *Z. Naturforsch. B* **1985**, *40*, 895–899.
(23) Abrahams, S. C.; Grison, E. *Acta Crystallogr.* **1953**, *6*, 206–213.
(24) Hordvik, A.; Sletten, E. *Acta Chem. Scand.* **1968**, *22*, 3029–&.
(25) Hulliger, F.; Siegrist, T. *Z. Naturforsch., B: J. Chem. Sci.* **1981**, *36*, 14–15.
(26) Schnerin, Hg; Goh, N. K. *Naturwissenschaften* **1974**, *61*, 272–272.
(27) Li, J.; Guo, H. Y.; Carey, J. R.; Mulley, S.; Proserpio, D. M.; Sironi, A. *Mater. Res. Bull.* **1994**, *29*, 1041–1048.
(28) Cordier, G.; Schwidetzky, C.; Schafer, H. *Z. Naturforsch., B: J. Chem. Sci.* **1984**, *39*, 833–834.
(29) Shoemaker, D. P.; Chung, D. Y.; Mitchell, J. F.; Bray, T. H.; Soderholm, L.; Chupas, P. J.; Kanatzidis, M. G. *J. Am. Chem. Soc.* **2012**, *134*, 9456–9463.
(30) Kanatzidis, M. G.; Huang, S. P. *Inorg. Chem.* **1989**, *28*, 4667–4669.
(31) Emirdag, M.; Schimek, G. L.; Kolis, J. W. *J. Chem. Crystallogr.* **1998**, *28*, 705–711.
(32) Jensen, W. B. *J. Chem. Educ.* **2003**, *80*, 952–961.
(33) Sommer, H.; Hoppe, R. *Z. Anorg. Allg. Chem.* **1978**, *443*, 201–211.
(34) Axtell, E. A.; Park, Y.; Chondroudis, K.; Kanatzidis, M. G. *J. Am. Chem. Soc.* **1998**, *120*, 124–136.
(35) Kanatzidis, M. G.; Park, Y. *Chem. Mater.* **1990**, *2*, 99–101.
(36) Klepp, K. O. *J. Alloy. Compd.* **1992**, *182*, 281–288.
(37) Li, J.; Chen, Z.; Lam, K. C.; Mulley, S.; Proserpio, D. M. *Inorg. Chem.* **1997**, *36*, 684–687.
(38) Klepp, K. O.; Prager, K. *Z. Naturforsch., B: J. Chem. Sci.* **1992**, *47*, 491–496.
(39) Rad, H. D.; Hoppe, R. *Z. Anorg. Allg. Chem.* **1981**, *483*, 18–25.
(40) Rad, H. D.; Hoppe, R. *Z. Anorg. Allg. Chem.* **1981**, *483*, 7–17.
(41) Sheldrick, G. M., *SHELXTL;* University of Goettingen: Goettingen, Germany, 1997.
(42) Mccarthy, T. J.; Ngeyi, S. P.; Liao, J. H.; Degroot, D. C.; Hogan, T.; Kannewurf, C. R.; Kanatzidis, M. G. *Chem. Mater.* **1993**, *5*, 331–340.
(43) Blochl, P. E. *Phys. Rev. B* **1994**, *50*, 17953–17979.
(44) Kresse, G.; Hafner, J. *J. Phys.: Condens. Mater.* **1994**, *6*, 8245–8257.
(45) Kresse, G.; Furthmuller, J. *Phys. Rev. B* **1996**, *54*, 11169–11186.
(46) Perdew, J. P.; Burke, K.; Ernzerhof, M. *Phys. Rev. Lett.* **1996**, *77*, 3865–3868.
(47) Marking, G. A.; Hanko, J. A.; Kanatzidis, M. G. *Chem. Mater.* **1998**, *10*, 1191–1199.
(48) Janz, G. J.; Coutts, J. W.; Downey, J. R.; Roduner, E. *Inorg. Chem.* **1976**, *15*, 1755–1758.
(49) Verhoeven, J. A. T.; Vandoveren, H. *Appl. Surf. Sci.* **1980**, *5*, 361–373.
(50) Zylberajchantoine, C.; Barraud, A.; Roulet, H.; Dufour, G. *Appl. Surf. Sci.* **1991**, *52*, 323–327.
(51) Smart, R. S.; Skinner, W. M.; Gerson, A. R. *Surf. Interface Anal.* **1999**, *28*, 101–105.
(52) Pratt, A. R.; Muir, I. J.; Nesbitt, H. W. *Geochim. Cosmochim. Acta* **1994**, *58*, 827–841.
(53) Vasquez, R. P. *J. Electron Spectrosc. Relat. Phenom.* **1991**, *56*, 217–240.
(54) Perdew, J. P.; Levy, M. *Phys. Rev. Lett.* **1983**, *51*, 1884–1887.
(55) Perdew, J. P.; Chevary, J. A.; Vosko, S. H.; Jackson, K. A.; Pederson, M. R.; Singh, D. J.; Fiolhais, C. *Phys. Rev. B* **1992**, *46*, 6671–6687.
(56) (a) Adel, J.; Weller, F.; Dehnicke, K. *Z. Naturforsch., B: J. Chem. Sci.* **1988**, *43*, 1094–1100. (b) Haushalter, R. C. *Angew. Chem., Int. Ed.* **1985**, *24*, 432–433.